Entropy Production During Laser Picosecond Heating of Copper

Bekir Sami Yilbas
King Fahd University of Petroleum and Minerals,
Dhahran 31261, Saudi Arabia

Nonequilibrium energy transport taking place in the surface region of the metallic substrate due to laser short-pulse heating results in entropy production in electron and lattice systems. The entropy analysis gives insight into the irreversible processes taking place in this region during the laser short-pulse heating process. In the present study, entropy production during laser shortpulse heating of copper is considered. Equations governing the nonequilibrium energy transport are derived using an electron kinetic theory approach. The entropy equations due to electron and lattice systems and coupling of these systems are formulated. The governing equations of energy transport and entropy production are solved numerically. Two pulse shapes, namely step input intensity and exponential intensity, are employed in the analysis. It is found that entropy production due to coupling process attains higher values than those produced due to electron and lattice systems. The effect of pulse shape on the entropy production inside the substrate material is significant.
[DOI: 10.1115/1.1488173]

1 Introduction

Laser shortpulse heating of metallic substrates initiates a nonequilibrium thermodynamic process taking place in the region irradiated by a laser beam. As the duration of the heating pulse becomes comparable to the thermalization time ($\tau_s = G/C_e \sim 10^{-13}$ s for most metals), nonequilibrium energy transport occurs during electron lattice site collisions. In this case, photons reaching the surface of metallic substrates interact with electrons in the conduction band and are absorbed, leaving the electrons with increased energies. The excited electrons make collisions with lattice site and transfer some of their excess energy to lattice site through the successive collisions. Since the energy absorbed by electrons is higher than energy being transferred to lattice site, electron temperature exceeds the lattice site temperature. As the heating progresses within the time domain of the electron thermalization time, electron temperature well excess of lattice site temperature is resulted in the surface region of the substrate material. Consequently, a micro-scale analysis of the heating process is essential to describe the energy transport process inside the substrate material.

Considerable research studies were carried out to explore the micro-scale energy transport, particularly, during the laser shortpulse heating process. A transient nonequilibrium temperature difference between electrons and lattice was investigated by Fujimoto et al. [1] for femtosecond laser interaction with metallic tungsten. They showed that electron-phonon energy relaxation time of several hundred femtoseconds occurred. Electron-phonon relaxation in copper due to shortpulse heating was studied by Elsayed-Ali et al. [2]. They observed nonequilibrium electron and lattice temperatures during the heating pulse. The generation of nonequilibrium electron and lattice temperatures in copper was studied by Eesley [3] through thermoreflectance measurements. He introduced two-equation heating model to correlate the measurement results. Femtosecond laser heating of multi-layer metals was analyzed by Qiu and Tien [4]. They showed that multi-layer metals presented very different thermal response from single-layer metals during the heating process. Electron temperature measurement in a highly excited gold target was carried out using a thermionic emission detection by Wang et al. [5]. They showed that the thermal conductivity, specific heat and electron-phonon coupling are temperature dependent for a highly excited electron-lattice system. A unified field approach for heat conduction from macro to micro scales was introduced by Tzou [6]. The universal form of the energy equation was shown to facilitate from one mechanism to another such as diffusion or wave to phonon-electron interaction. A simplified approach was introduced by Al-Nimr and Arpaci [7] to describe the thermal behavior of a thin metal film exposed to picosecond thermal pulses. The proposed approach eliminated the coupling between the energy equations for the condition $GL^2/Ke \gg 1$, where G is the coupling factor, L is the thickness, and Ke is the thermal conductivity. Yilbas [8] introduced an electron kinetic theory approach to model the microscale heating process. The analysis was based on the energy transport through electron lattice site collisions. Moreover, Yilbas and Shuja [9] showed that electron kinetic theory, two-equation model and the Fourier theory results converged as the heating period exceed to nanosecond durations.

In nonequilibrium process, the physical parameters are thermodynamically imbalance resulting in nonequilinrium thermodynamic potential. The coupling of these physical parameters results in irreversible processes taking place in the thermal system. The irreversible processes produce entropy, which depends on the all thermodynamic potentials (forces) and fluxes generated in the thermal system. The driving force for entropy production is controlled by the coupling of the physical parameters, which include temperature, mass transfer rate, pressure differential, etc. Considerable research studies were carried out to explore the entropy generation in nonequilibrium thermodynamic systems. The irreversible extension of the Carnot cycle of maximum mechanical work delivered from a system of finite-resources was investigated by Sieniutycz [10]. He demonstrated that bounds of the classical availability should be replaced by stronger bounds obtained for finite time processes. A drying process in a heterogeneous multiphase system based on nonequilibrium thermodynamic model was studied by Menshutine and Darokhov [11]. Linear-nonequilibrium thermodynamic model for coupled heat and mass transport processes was examined by Demirel and Sandler [12]. They expressed the phenomenological equations with the resistance coefficients that were capable of reflecting the extend of the interactions between heat and mass flows. Yilbas [13] introduced the entropy number for laser pulse heating process. The entropy analysis was based on the equilibrium thermodynamics, since the heating duration was in the order of nanoseconds (which is greater than the thermalization time). In the case of laser short-pulse heating process, nonequilibrium energy transport occurs and this de-

Contributed by the Advanced Energy Systems Division for publication in the JOURNAL OF ENERGY RESOURCES TECHNOLOGY. Manuscript received by the AES Division, March 24, 2001; revised manuscript received April 5, 2002. Associate Editor: S. Garimella.

pends on the degree of coupling between electrons and lattice site during the successive collisions. Consequently, in laser shortpulse heating process, nonequilibrium thermodynamic analysis should be considered when formulating the entropy production during the heating pulse.

The entropy analysis gives insight into the irreversible processes taking place in the thermal system. Moreover, the entropy analysis provides information on the nonequilibrium thermodynamic potentials during the thermal communication of electron and lattice systems. Consequently, in the present study, the extension of the previous work [13] was considered and the entropy analysis during nonequilibrium energy transport due to laser shortpulse heating is carried out. The governing equations of entropy production are formulated using the nonequilibrium thermodynamic aspects. In the analysis variable thermophysical properties are employed.

2 Mathematical Analysis of Heating Process

2.1 Electron Kinetic Theory Approach. The electron kinetic theory approach considers the electron-phonon collision mechanism through which the energy exchange between the electrons and lattice site atoms occur. The mathematical model pertinent to electron kinetic approach is given in the previous study [8] and [9], hence, the basics of the analysis are given here.

The number of electrons which have just collided in ds during dt before colliding in dx is

$$N_{sx}A\overline{V}dt\frac{ds}{\lambda}\frac{dx}{\lambda}\exp\left(-\frac{|x-s|}{\lambda}\right)$$

where $ds/\lambda dx/\lambda \exp(-|x-s|/\lambda)$ is the electrons—lattice site atoms collision probability as described in [8].

If the temperature of the lattice site atoms in dx is $T_l(x,t)$ and the temperature of the electrons when they arrive at dx is $T_e(s,t)$, then the energy transfer to the lattice site atoms in dx from collisions with electrons in which the electrons give up a fraction "f" of their excess energy is

$$N_{sx}A\overline{V}dt\frac{ds}{\lambda}\frac{dx}{\lambda}\exp\left(-\frac{|x-s|}{\lambda}\right)fk_B[T_e(s,t)-T_l(x,t)]$$

The fraction of electron excess energy transfer during the time comparable or greater than the relaxation time (τ_s) can be written in terms of the energy balance across the section dx in the substrate material; i.e.

$$f=\frac{(\text{Electron energy})_{\text{in}}-(\text{Electron energy})_{\text{out}}}{(\text{Electron energy})_{\text{in}}-(\text{Phonon Energy})}$$

or

$$f=\frac{(T_e)_{\text{in}}-(T_e)_{\text{out}}}{(T_e)_{\text{in}}-T_l} \tag{1}$$

where $(T_e)_{\text{in}}$ is the temperature of an electron entering the section, $(T_e)_{\text{out}}$ temperature of the an electron leaving the section, and T_l is the phonon temperature. f takes the values $0\leqslant f\leqslant 1$.

Summing the contribution from all such sections as to the energy gives

$$\Delta E=Adxdt\int_{-\infty}^{\infty}\frac{N_{sx}\overline{V}fk_B}{\lambda^2}\exp\left(-\frac{|x-s|}{\lambda}\right)[T_e(s,t)-T(x,t)]ds \tag{2}$$

The total amount of energy which is absorbed in an element $\partial\xi$, area A in time dt is

$$-I_oAdtd\xi f'(\xi)$$

since all the beam energy is absorbed in the x direction.

The electron densities may vary throughout the material and, in particular, the number traveling from ds to dx may not be the same as that from dx to ds. Therefore, the total amount absorbed by this electron from dx to ds is

$$\int_x^s I_o\frac{d\xi f'(\xi)}{(N_{sx}+N_{xs})V} \tag{3}$$

Equation (3) gives extra energy obtained by the electron in travelling from ds to dx. Substitution of Eq. (3) into Eq. (2) results the expression for the change of energy of the lattice site atoms in the section

$$\frac{\Delta E}{Adxdt}=\int_{-\infty}^{\infty}\frac{N_{sx}\overline{V}fk_B}{\lambda^2}\exp\left(-\frac{|x-s|}{\lambda}\right)[T_e(s,t)-T_l(x,t)]ds + \int_{-\infty}^{\infty}\frac{I_of}{\lambda^2}\frac{N_{sx}}{N_{sx}+N_{xs}}\exp\left(-\frac{|x-s|}{\lambda}\right)\int_x^s f'(x)d\xi ds \tag{4}$$

Since the energy which is transferred to the lattice site atoms in this collision process results in a change of both potential and vibration energy, then

$$\frac{\Delta E}{Adxdt}=\frac{Adx}{Adxdt}\Delta[NM(U_o+3k_BT_l(x,t))]$$

The energy stored during a infinitely small time interval δt in the substrate is

$$\frac{\Delta E}{\delta t}=\frac{E(t+\delta t)-E(t)}{\delta t} \tag{5}$$

Expanding Eq. (5) using a Taylor series, it yields

$$\frac{\Delta E}{\delta t}=\frac{1}{\delta t}\left[E(t)+\delta tE'(t)+\frac{(\delta t)^2}{2!}E''(t)+\ldots-E(t)\right]$$

or

$$\Delta E=E'(t)+\frac{(\delta t)}{2!}E''(t)+\ldots \tag{6}$$

where ΔE is the energy content. The energy content of the substrate in a section dx apart can also be written as

$$\Delta E=Adx\rho CpT(x,t) \tag{7}$$

Therefore, substitution of Eq. (7) into Eq. (6) gives

$$\frac{\Delta E}{\delta t}=Adx\left[\frac{\partial}{\partial t}(\rho CpT_l(x,t))+\frac{(\delta t)}{2!}\frac{\partial^2}{\partial t^2}(\rho CpT_l(x,t))+\ldots\right] \tag{8}$$

For per unit area and distance, and when the time step approaches and becomes greater than the thermal relaxation time, Eq. (8) reduces to

$$\frac{\Delta E}{Adxdt}\approx\frac{\partial}{\partial t}(\rho CpT_l(x,t))+\tau_s\frac{\partial^2}{\partial t^2}(\rho CpT_l(x,t)) \tag{9}$$

where τ_s is the thermal relaxation time. Therefore, the complete equation for the electron—lattice site atom collision process is

$$\frac{\partial}{\partial t}\left[(\rho CpT_l(x,t))+\tau_s\frac{\partial}{\partial t}(\rho CpT_l(x,t))\right]$$
$$=\int_{-\infty}^{\infty}\frac{N_{sx}\overline{V}fk_B}{\lambda^2}\exp\left(-\frac{|x-s|}{\lambda}\right)T_e(s,t)ds$$
$$-\int_{-\infty}^{\infty}\frac{N_{sx}\overline{V}fk_B}{\lambda^2}\exp\left(-\frac{|x-s|}{\lambda}\right)T_l(x,t)ds$$
$$+\int_{-\infty}^{\infty}\frac{I_of}{\lambda^2}\frac{N_{sx}}{N_{sx}+N_{xs}}\exp\left(-\frac{|x-s|}{\lambda}\right)\int_x^s f'(x)d\xi ds \quad (10)$$

The final temperature of the electrons in dx after the collision process can be readily found from the conservation of energy; i.e., *total electron energy after collision=total electron energy in during dt−change of lattice site energy*. Total electron energy after collision

$$\int_{-\infty}^{\infty}\frac{N_{sx}\overline{V}(1-f)k_B}{\lambda^2}\exp\left(-\frac{|x-s|}{\lambda}\right)T_e(s,t)ds \quad (11)$$

Total electron energy carried into dx during dt is

$$\int_{-\infty}^{\infty}\frac{N_{sx}\overline{V}k_B}{\lambda^2}\exp\left(-\frac{|x-s|}{\lambda}\right)\theta(s,t)ds+\int_{-\infty}^{\infty}\frac{I_of}{\lambda^2}\frac{N_{sx}}{N_{sx}+N_{xs}}$$
$$\times\exp\left(-\frac{|x-s|}{\lambda}\right)\int_x^s f'(x)d\xi ds \quad (12)$$

and the change of lattice site atom energy is

$$\frac{\partial}{\partial t}\left[\rho CpT_l(x,t)+\tau_s\rho Cp\frac{\partial}{\partial t}(T_l(x,t))\right]$$

as given by Eq. (9). Consequently, substituting the Eqs. (10)–(12) into the requirement of the conservation of energy gives

$$\int_{-\infty}^{\infty}\frac{N_{sx}\overline{V}k_B}{\lambda^2}\exp\left(-\frac{|x-s|}{\lambda}\right)[T_e(s,t)-fT_l(x,t)]ds$$
$$=\int_{-\infty}^{\infty}\frac{N_{sx}\overline{V}k_B}{\lambda^2}\exp\left(-\frac{|x-s|}{\lambda}\right)(1-f)\theta(s,t)ds$$
$$+\int_{-\infty}^{\infty}(1-f)\frac{N_{sx}}{N_{sx}+N_{xs}}\exp\left(-\frac{|x-s|}{\lambda}\right)\int_x^s f'(x)d\xi ds \quad (13)$$

Equations (10) and (13) have been kept, in general; however, it may be useful to consider a particular case where electrons cannot escape through the surface (which may equally apply when a steady-state space charge exists). In this case, the assumption that all directions of travel are equally probable gives

$$N_{sx}=N_{xs}=\frac{N}{3}$$

where N is the number of free electrons per unit volume. In this case, Eqs. (10) and (13) yield

$$\frac{\partial}{\partial t}\left[\rho CpT_l(x,t)+\tau_s\frac{\partial}{\partial t}(\rho CpT_l(x,t))\right]$$
$$=\int_{-\infty}^{\infty}\frac{f}{\lambda^3}\exp\left(-\frac{|x-s|}{\lambda}\right)T_e(s,t)ds$$
$$-\int_{-\infty}^{\infty}\frac{fk}{\lambda^3}\exp\left(-\frac{|x-s|}{\lambda}\right)T_l(x,t)ds$$
$$+\int_{-\infty}^{\infty}\frac{I_of}{\lambda^2}\exp\left(-\frac{|x-s|}{\lambda}\right)\int_x^s f'(x)d\xi ds \quad (14)$$

which makes use of the simple kinetic theory result for the thermal conductivity

$$k=\frac{N\overline{V}k_B\lambda}{3}$$

and

$$\left[\int_{-\infty}^{\infty}\frac{k}{\lambda^3}\exp\left(-\frac{|x-s|}{\lambda}\right)[T_e(s,t)-fT_l(x,t)]ds\right]$$
$$=\int_{-\infty}^{\infty}\frac{k}{\lambda^3}\exp\left(-\frac{|x-s|}{\lambda}\right)(1-f)T_e(s,t)ds$$
$$+\int_{-\infty}^{\infty}(1-f)\exp\left(-\frac{|x-s|}{\lambda}\right)\int_x^s f'(x)d\xi ds \quad (15)$$

Equations (14) and (15) are the equations of interest for laser short-pulse heating process. The method of solution to be used in the following analysis is the transformation of the simultaneous differential—integral equations (14) and (15) using the Fourier integral transformation, with respect to x [14]. Since the mathematical arrangements of the Fourier transformation are given in the previous study, the resulting equation is given here; i.e.

$$\left[f\left(1+\tau_s\frac{\partial T_l}{\partial t}\right)-\frac{\lambda^2\partial^2}{\partial x^2}\right]\rho Cp\frac{\partial T_l}{\partial t}=kf\frac{\partial^2 T_l}{dx^2}+I_o\delta f\exp(-\delta|x|) \quad (16)$$

If the terms $\lambda^2/f\partial^2/\partial x^2(\rho Cp\partial T_l/\partial t)$ and $f\tau_s\partial/\partial t(\rho Cp\partial T_l/\partial t)$ are neglected for all f values, Eq. (16) becomes

$$\rho Cp\frac{\partial T_l}{\partial t}=k\frac{\partial^2 T_l}{dx^2}+I_o\delta\exp(-\delta|x|)$$

which is the same as a Fourier heat conduction equation. Equation (16) can be rewritten as

$$\rho Cp\frac{\partial T_l}{\partial t}=k\frac{\partial^2 T_l}{dx^2}+f\frac{\lambda^2\partial^2}{\partial x^2}\left(\rho Cp\frac{\partial T_l}{\partial t}\right)-\rho Cp\tau_s\frac{\partial^2 T_l}{\partial t^2}$$
$$+I_o\delta\exp(-\delta|x|) \quad (17)$$

When Eq. (17) is decomposed into two equations, the resulting differential equations can be written as

$$A\frac{\partial T_e}{\partial t}=B\frac{\partial^2 T_e}{dx^2}-C[T_e-T_l]+I_o\delta\exp(-\delta|x|)$$
$$D\frac{\partial T_l}{\partial t}=C[T_e-T_l] \quad (18)$$

To find the values of A, B, C, and D, the following procedure is adopted; i.e.:

$$D\frac{\partial^2 T_l}{\partial t^2}=C\left[\frac{\partial T_e}{\partial t}-\frac{\partial T_l}{\partial t}\right]$$

or

$$\frac{\partial T_e}{\partial t} = \frac{D}{C}\frac{\partial^2 T_l}{\partial t^2} + \frac{\partial T_l}{\partial t} \tag{19}$$

Similarly

$$D\frac{\partial^2}{\partial x^2}\left(\frac{\partial T_l}{\partial t}\right) = C\left[\frac{\partial^2 T_e}{\partial x^2} - \frac{\partial^2 T_l}{\partial x^2}\right]$$

or

$$\frac{\partial^2 T_e}{\partial x^2} = \frac{D}{C}\frac{\partial^2}{\partial x^2}\left(\frac{\partial T_l}{\partial t}\right) + \frac{\partial^2 T_l}{\partial x^2} \tag{20}$$

Substitution of Eqs. (19) and (20) into Eq. (17) yields

$$(D+A)\frac{\partial T_l}{\partial t} = \frac{BD}{C}\frac{\delta^2}{\partial x^2}\left(\frac{\partial T_l}{\partial t}\right) + B\frac{\partial^2 T_l}{\partial x^2} - \frac{AD}{C}\frac{\partial^2 T_l}{\partial t^2} + I_o\delta\exp(-\delta|x|) \tag{21}$$

After equation Eqs. (21) and (17), the coefficients *A*, *B*, *C*, and *D* can be calculated; i.e.

$$A = \frac{fk\tau_s}{\lambda^2}$$

$$B = k$$

$$C = \frac{fk}{\lambda^2}\left(1 - \frac{k\tau_s}{\rho Cp\lambda^2}\right)$$

$$D = \rho Cp - \frac{fk\tau_s}{\lambda^2}$$

Equation (19) is identical to equations given in the two-equation model, since the governing equations in two-equation model is [3]

$$C_e\frac{\partial T_e(s,t)}{\partial t} = \nabla(kT_e(s,t)) - G[T_e(s,t) - T_l(x,t)] + S$$

and

$$C_l\frac{\partial T_l(x,t)}{\partial t} = G[T_e(s,t) - T_l(x,t)] \tag{22}$$

$T_e(s,t)$ and $T_l(x,t)$ are the electron and lattice site temperatures, S is the laser source term ($I_o\delta\exp(-\delta x)$), and C_e and C_l are the electron and lattice heat capacities, respectively. G is the electron-phonon coupling factor, given by

$$G = \frac{\pi^2 m_e N\overline{V}^2}{6\tau_p T_e(s,t)}$$

where m_e, N, $\overline{V}$, and τ_p are electron mass, electron number density, electron drift velocity and the electron mean free time between electron-phonon coupling respectively. Consequently, setting the coefficients of Eqs. (19) and (22), it yields

$$\frac{fk\tau_s}{\lambda^2} = Ce$$

$$\frac{fk}{\lambda^2}\left(1 - \frac{k\tau_s}{\rho Cp\lambda^2}\right) = G$$

$$\rho Cp - \frac{fk\tau_s}{\lambda^2} = C_l$$

where $\tau_s = G/C_e$ (Fujimoto) and $C_e = \gamma T_e$ [1,15]. Moreover, the electron phonon coupling factor is electron temperature dependent, which can be written as [3]

$$G = \frac{\pi^2 mN\overline{V}^2}{6\tau_s T_l}\left(\frac{T_e}{T_l}\right)^4 \int_0^{T_e/T_d} \frac{x^4}{e^x - 1}dx \tag{23}$$

Using the relation $fk\tau_s/\lambda^2 = Ce$, the electron mean free path becomes

$$\lambda = \sqrt{\frac{fk\tau_s}{Ce}} \tag{24}$$

Since $C_e = \gamma T_e$ (where γ is constant and $\gamma = 69.9$ J/m^{3}K^2 for copper [3]).

2.2 Entropy Analysis. The nonequilibrium energy transport process results in different temperatures of electron and lattice site in the substrate material. In this case, substrate material can be considered as consisting of two systems with two different temperatures, provided that the two systems are thermally in contact. Consequently, in the present study the entropy analysis is based on the two systems having different temperatures and thermally in contact.

When two thermal systems with different temperatures (T_A and T_A) are in contact and nonequilibrium energy transport takes place between the systems, then the entropy production can be written as [16]

$$\Delta S_{AB} = \frac{\delta Q_A}{T_A} + \frac{\delta Q_B}{T_B} + \delta Q_{AB}\left(\frac{1}{T_A} + \frac{1}{T_B}\right) \tag{25}$$

where *A* and *B* correspond to first and second systems in contact, respectively. δQ_A, δQ_B, and δQ_{AB} are the heat transfer to systems *A* and *B*, and heat transfer occurring inside the combined system *A* and *B*, respectively. The first two terms in Eq. (25) represent entropy change, due to the equilibrium conditions, for the systems *A* and *B*, while the third term ($\delta Q_{AB}(1/T_A + 1/T_B)$) represents the irreversible entropy generation inside the systems boundary due to coupling of the systems. Therefore, for electron and lattice systems, entropy production rate can be written as the sum of entropy production due to electron and lattice systems, and the entropy production due to contribution of electron and lattice system coupling. In this case, entropy production rate during the nonequilibrium energy transport process can be written as

$$\dot{s}_t = \dot{s}_e + \dot{s}_l + \dot{s}_{el} \tag{26}$$

and

$$\dot{s}_{el} = \chi J_q$$

where $\dot{s}_t, \dot{s}_e, \dot{s}_l, \dot{s}_l(\chi J_q)$ are total entropy production rate, electron system entropy production rate, lattice system entropy production rate, and coupling process (coupling between electron and lattice system) entropy production rate, respectively. χ and J_q represent the thermodynamic potential (driving potential energy underlying entropy production) and flux components in the coupling process [16]. It should be noted that the entropy production rate due to coupling process (last term in Eq. (25)) is modeled using the thermodynamic potential and flux components in the coupling process. The contribution of χJ_q is due to the irreversibility associated with the nonequilibrium thermodynamic process taking place in electron lattice coupled system. The entropy production in the electronic and lattice systems can be formulated through statistical thermodynamics analysis. The entropy of the oscillators in the thermal system can be written as

$$s_{ent} = k_B \ln W$$

where k_B is the Boltzmann's constant and W is the summation of the overall microscopic distribution of the oscillators. Using the Stirling formula, the logarithmic form of the distribution can be written as [16]

$$\ln W = \sum_i N_j\left[k_B\left(\frac{gj}{N_j}\right) + 1\right]$$

where N and g_j are the number of oscillators and number of quantum states, respectively. From the most probable distribution

$$\frac{g_j}{N_j}=\frac{Z}{N}e^{-\epsilon_i/k_BT}$$

where Z is a partion function, which is

$$Z=\sum_j g_j e^{-\epsilon_i/k_BT}$$

Therefore

$$\ln W=\ln\frac{Z}{N}\sum_j N_j+\frac{1}{k_BT}\sum_j N_j\epsilon_j+\sum_j N_j$$

or

$$\ln W=N\ln\frac{Z}{N}+\frac{u}{k_BT}+N$$

Using Stirling's formula, the entropy production becomes

$$s_{\text{ent}}=k_B\ln Z_n+\frac{u}{T} \tag{27}$$

where

$$Z_n=\frac{Z^N}{N!}$$

Therefore, the entropy production rate per oscillator becomes

$$\dot{s}_{\text{ent}}=\frac{d}{dt}\left[k_B\ln Z_n+\frac{u}{T}\right] \tag{28}$$

The entropy production rate for N oscillator can be written as

$$\dot{s}_{\text{ent}}=\frac{d}{dt}\left[N\left(k_B\ln Z_n+\frac{u}{T}\right)\right]$$

However, the entropy production at time interval $\Delta\tau$ during the heating pulse can be written as:

$$s_{\text{ent}}=\int_0^{\Delta\tau}\dot{s}_{ent}dt \tag{29}$$

Equation (29) is used to determine the entropy production due to electron and lattice systems.

In the case of a coupling process, nonequilibrium contribution of the entropy production needs to be formulated in terms of thermodynamic potential (potential energy) and flux relation [16]. The driving potential energy underlying entropy production, due to nonequilibrium energy transport, during the irreversible process can be written as [16]

$$\chi=\Delta\left(\frac{1}{T}\right) \tag{30}$$

The energy flux through the collisional process per unit volume and per unit time can be written as

$$\frac{\Delta E}{Adxdt}=\frac{d}{dt}[Nk_B(T_e-T_l)]$$

The energy flux per unit time is

$$J_q=\frac{\Delta E}{Adxdt}$$

or

$$J_q=\frac{d}{dt}[Nk_B(T_e-T_l)] \tag{31}$$

Therefore, the entropy production rate due to coupling process is

$$\dot{s}_{el}=\Delta\left(\frac{1}{T}\right)\frac{d}{dt}[Nk_B(T_e-T_l)]Adx \tag{32}$$

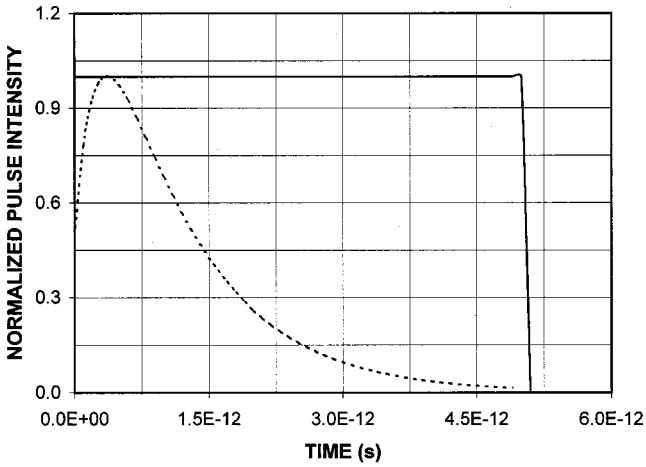

Fig. 1 Normalized pulse intensity for two pulse shapes

The entropy production due to coupling process at time interval $\Delta\tau$ during the heating pulse can be written as

$$s_{el}=\int_0^{\Delta\tau}\dot{s}_{el}dt \tag{33}$$

Equation (33) is used to determine entropy production due to coupling process. The spatially integrated entropy production at time interval $\Delta\tau$ during the heating pulse can be written as

$$(s_{\text{ent}})_{\text{Integ}}=\int_0^{\infty}s_{el}dx \tag{34}$$

2.3 Numerical Solution. The numerical method employed uses a finite difference scheme, which is well established in the literature [17]. In order to obtain accurate results, the convergency criteria should be met. The stability criteria for the heating model is as follows:

$$1\geqslant\text{ABS}\left[\frac{f\rho Cp}{\Delta t}+2\lambda^2\rho Cp\left[\frac{1}{\Delta t(\Delta x)^2}\right]-2kf\left[\frac{1}{(\Delta x)^2}\right]\right]+\text{ABS}\left[\frac{kf}{(\Delta x)^2}-\frac{2\lambda^2\rho Cp}{\Delta t(\Delta x)^2}\right]+ABS\left[\frac{2\lambda^2\rho Cp}{\Delta t(\Delta x)^2}\right]-\text{ABS}\left\{\frac{f\rho Cp}{\Delta t}+2\lambda^2\rho Cp\left[\frac{1}{\Delta t(\Delta x)^2}\right]\right\}$$

where Δx is spatial increments in the x axis while Δt is the time increment.

In order to account for the exponential pulse shape, a mathematical function resembling the exponential pulse shape is introduced; i.e.

$$I=I_o[\exp(-\beta t)-\exp(-\gamma t)]$$

Figure 1 shows the exponential and step input pulse intensities, while thermophysical properties of copper and laser pulse properties used in the computations are given in Tables 1 and 2.

3 Results and Discussion

Entropy production in copper during a laser shortpulse heating process is considered. The substrate material is assumed as composing of two thermal systems, namely electron and lattice systems, with different temperatures after the initiation of nonequilibrium energy transport process. The assumption enables to introduce the entropy production of individual system as well as the entropy production due to energy coupling between electron

Table 1 Thermal properties of copper at 100 and 300 K [3]

T_e	T_d	$\delta\times10^7$	$m\times10^{-31}$	$C_l\times10^6$	k	$G\times10^{16}$	$C_e\times10^4$	τ_s	$N\times10^{28}$
K	K	(1/m)	(kg)	(J/Km^3)	(W/mK)	(W/m^3K)	(J/Km^3)	(ps)	$1/m^{-3}$
100	343	7.1	9.1	2.26	610	8.6	0.966	0.7439	8.4
300	343	7.1	9.1	8.43	401	26	2.90	0.7439	8.4

and lattice systems. Consequently, entropy production due to individual system as well as the contribution of the coupling process are discussed here.

In order to compare the coefficients (*A*, *B*, *C*, and *D*) in Eq. (18) with the coefficients of differential equations in two equation model (Eq. (22)), Table 3 is developed for electron temperature 300 K. The values of coefficients corresponding to the two-equation model agree well with the computed values of *A*, *B*, *C*, and *D*. Consequently, Eqs. (18) and (22) should predict similar temperature profiles.

Figure 2 shows the entropy production of the electron system inside the substrate material at different heating periods. The entropy production increases and reaches a maximum in the surface vicinity of the substrate material. This is more pronounced in the heating period. This occurs because of the electron energy gain from the irradiated field, which can also be seen from electron temperature distribution inside the substrate material as shown in Fig. 3. In this case, electron temperature in the surface vicinity attains high values provided that electron temperature gradient variation ($\partial T_e/\partial x$) is small in this region. Moreover, next to the surface vicinity ($\sim 0.2\times10^{-8}$ m), electron temperature reduces sharply. Consequently, energy exchange in the region between the surface vicinity and next to it becomes considerable, which in turn increases the entropy production in this region. As the distance increases further from the surface towards the solid bulk, entropy production reduces. This is because of the excess energy gain of the electron system, which reduces in this region. When comparing Figs. 2(*a*) and (*b*), the entropy contours corresponding to step input intensity profile differs than those corresponding to exponential pulse profile. In this case, electrons gain considerable energy from the irradiated field in the early heating period and transfer only a small fraction of their excess energy to the lattice site through collisional process. Consequently, excess energy gain of the electron system increases at a higher rate for the step intensity pulse case as compared to its counterpart corresponding to the exponential pulse. The decay of entropy production curve along the depth from the surface of the substrate material changes at different heating periods. This is because of the energy absorption and transfer processes in the electron system.

Figure 4 shows the entropy production in the lattice system at different heating periods, and for two pulse intensity profiles. the

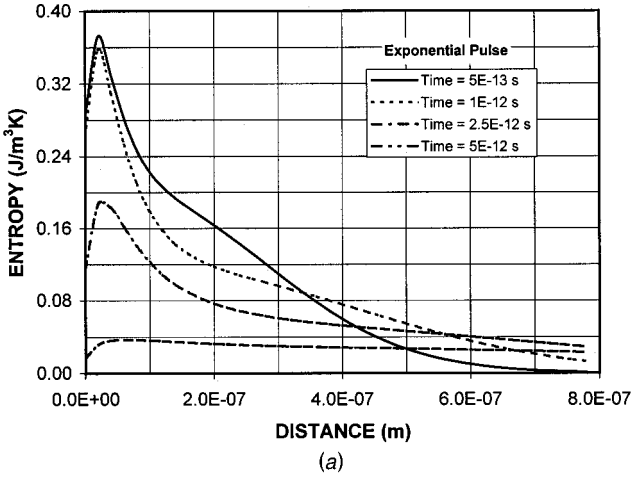

(*a*)

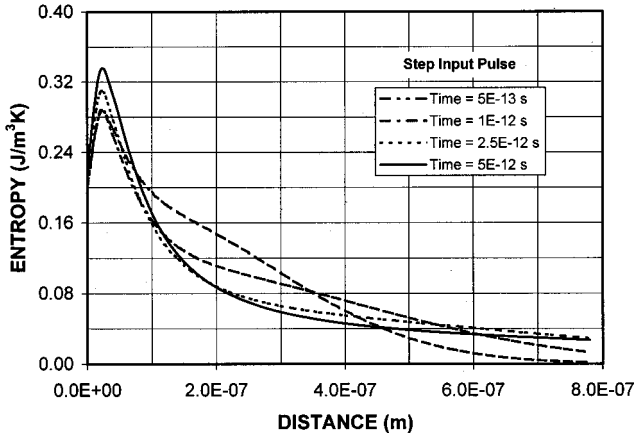

(*b*)

Fig. 2 Electron system entropy production inside the substrate material at different heating periods—(*a*) for exponential pulse shape, (*b*) for step input pulse shape

Table 2 The values of coefficients used in the simulations and laser pulse properties

λ	m	10^{-9}-10^{-10}
f		10^{-1}-10^{-5}
$A\times10^4$	(W/m^3K)	2.92 - 2.09
B	(W/mK)	401
$C\times10^{17}$	(W/m^3K)	3.12 - 2.49
$D\times10^6$	(J/m^3K)	8.57-2.49
β	1/s	10^{-12}
γ	1/s	4×10^{-12}
I_o (Exponential)	(W/m^2)	2.12×10^{12}
I_o (Step input)	(W/m^2)	10^{12}

Table 3 The coefficients *A*, *B*, *C*, and *D* and corresponding values in the two-equation model

$A\times10^4$ (J/m^3K)	$C_e\times10^4$ (J/m^3K)	$B\times10^4$ (W/mK)	k (W/mK)	$C\times10^{16}$ (W/m^3K)	$G\times10^{16}$ (W/m^3K)	$D\times10^{16}$ (J/m^3K)	$C_l\times10^6$ (J/m^3K)
8.44	8.43	401	401	25.76	26	2.86	2.90

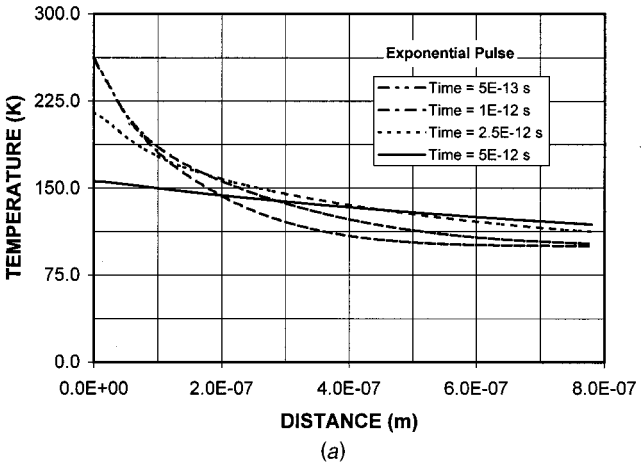

(*a*)

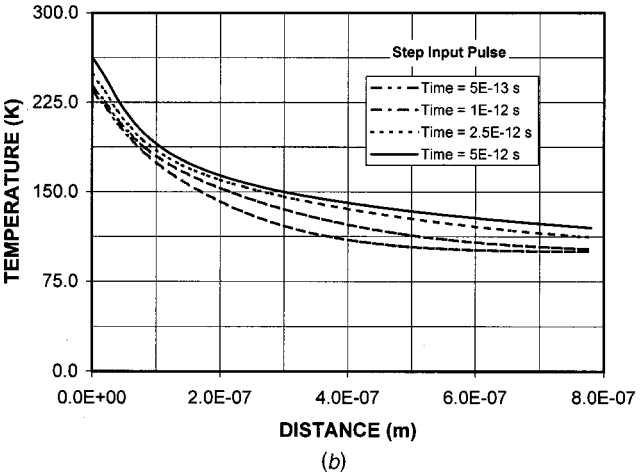

(*b*)

Fig. 3 Electron temperature inside the substrate material at different heating periods—(*a*) for exponential pulse shape, (*b*) for step input pulse shape

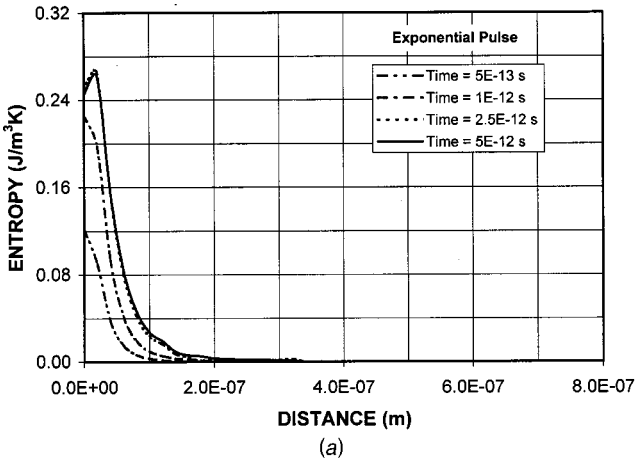

(*a*)

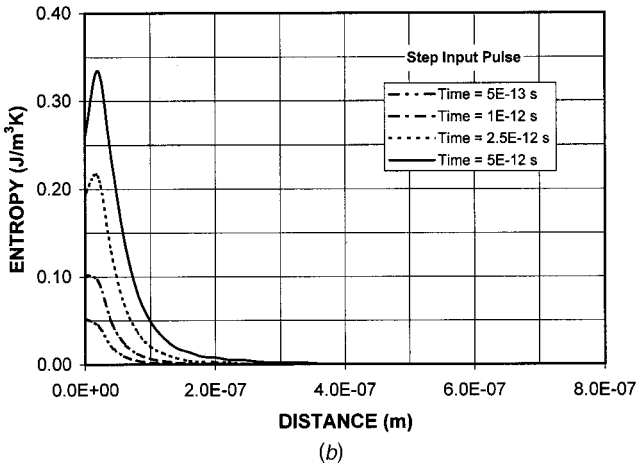

(*b*)

Fig. 4 Lattice system entropy production inside the substrate material at different heating periods—(*a*) for exponential pulse shape, (*b*) for step input pulse shape

entropy production increases and reaches a maximum in the surface vicinity of the substrate material as similar to the case for electron system. In this case, lattice site temperature increases in the surface vicinity, as seen from Fig. 5. The electron excess energy transfers to lattice site at a higher rate in the surface vicinity as compared to that at some depth below the surface, since the electron excess energy is high in the surface region. Consequently, energy gain of the lattice system is higher in the surface vicinity as compared to that at some depth below the surface. This enhances the entropy production in this region of the lattice system. The trend of the entropy production decay along the depth below the surface does not vary considerably for different heating periods. This is because of the small temperature rise in the lattice system during the short heating duration, as evident from Fig. 5. The effect of pulse profile on the entropy production is not considerable provided that the amount of entropy production is higher for the step input pulse as compared that corresponding to exponential pulse shape.

Figure 6 shows the entropy production inside the substrate material due to coupling process (coupling of electron and lattice systems) for different heating periods. As the heating progresses ($t \geqslant 2.5\times10^{-12}$ s), the entropy production attains high values in the surface vicinity and decays gradually as the distance from the surface extends towards the solid bulk of the substrate material. This is because of the sharp change in the potential energy component (χ) and the flux term (J_n) along the depth, i.e., electrons absorb less energy from the irradiated field as the depth from the surface increases (Lambert's law). Consequently, excess energy transfer from electrons to lattice site through collisional process becomes less as the depth increases. This results in less energy transferring (energy flux) from electron system to lattice system. Since the amount of energy gain by electrons from the irradiated field is less as well as energy transferred to lattice system is also less as depth increases. Consequently, the rise of temperature of electrons as well as lattice system become less at some depth below the surface. However, entropy production reduces sharply with depth in the early heating period ($t<2.5\times10^{-12}$ s). This occurs because of the potential energy component ($\Delta(1/T) = \Delta T/T_e T_i$), which attains very high values in the early heating period. Temperature difference between electrons and lattice site is small in the early heating period and their multiplication is also small. This in turn results in relatively large values of potential energy component than those corresponding to the later heating periods. The energy flux from electron system to lattice system increases for later heating periods, the potential energy component in the entropy production term becomes smaller as compared to its counterpart corresponding to early heating periods. Consequently, the amount of entropy production for the later heating period becomes lesser than that corresponding to the early heating period. The effect of pulse shape on the entropy production is significant. In this case, entropy production attains smaller values for step input intensity pulse than that corresponding to the exponential pulse. This is because of the potential energy component in the entropy production term such that it attains large values for the exponential pulse profile. It should be noted that step input pulse

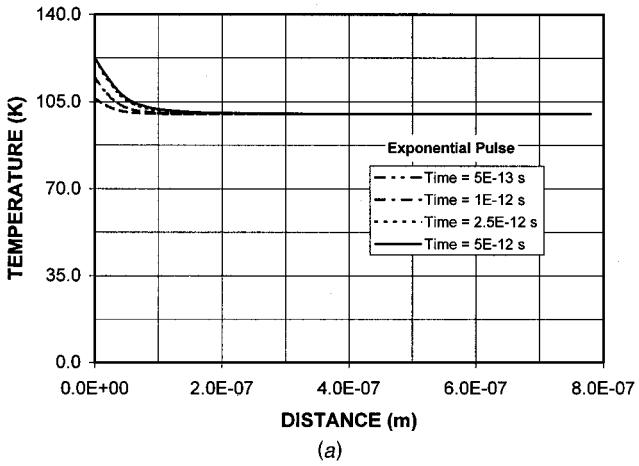

Fig. 5 Lattice site temperature inside the substrate material at different heating periods—(*a*) for exponential pulse shape, (*b*) for step input pulse shape

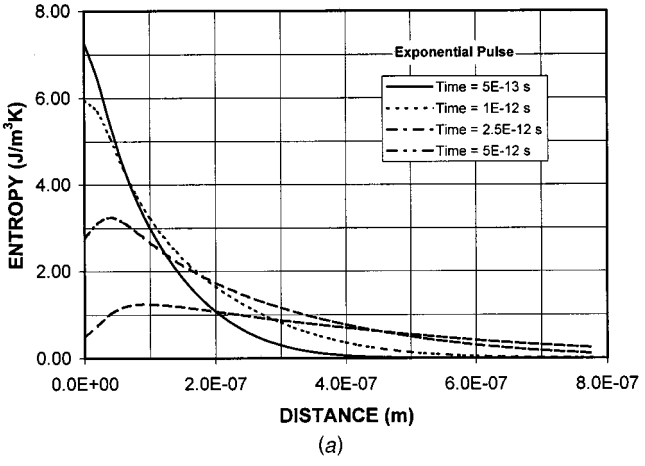

Fig. 6 Coupling process entropy production inside the substrate material at different heating periods—(*a*) for exponential pulse shape, (*b*) for step input pulse shape

results in high electron and lattice temperature, but the potential energy term ($\Delta(1/T)$) becomes small inside the substrate material.

Figure 7 shows the temporal variation of spatially integrated entropy production due to electron, lattice systems, and coupled process for two pulse shapes. The entropy production increases rapidly in the early heating period ($t \leqslant 0.75 \times 10^{-12}$ s) and the rate of entropy rise reduces as the heating period progresses. This is particularly true for the coupled process. The rapid rise of the entropy production rate is because of the rapid rise of electron and slow rise of lattice site temperatures. In this case, the potential energy component in the entropy production term increases in the early heating period. When comparing the entropy production due to electron and lattice systems with coupling process, the magnitude of the entropy production due to coupling process well exceeds the entropy production corresponding to electron and lattice systems. This is more pronounced as the heating progresses. The effect of pulse shape on the temporal behavior of the entropy production is very significant. In this case, the entropy production curve shows almost the same trend with the exponential pulse shape as shown in Fig. 1; i.e., entropy increases reaching a maximum and decays as the heating period progresses. However, step input pulse shape results in a paraboliclike behavior of the entropy production with time.

4 Conclusions

Entropy production during laser shortpulse heating of copper is considered. Since the nonequilibrium energy transport taking place in the surface region of the substrate material results in different electron and lattice site temperatures, the substrate material is considered composed of electron and lattice systems thermally in contact. In this case, entropy contribution of the coupling process between electron and lattice systems is also considered. Consequently, the governing equations of entropy production due to electron, lattice, and coupling processes are formulated for picosecond laser heating of copper. It is found that entropy production due to coupling process well exceeds its counterparts due to electron and lattice systems. The reason behind the large entropy production is the potential energy component and energy flux in the entropy production term, which attain considerably high values. The specific conclusions derived from the present study are listed as follows:

1. The entropy production due to electron system increases to reach maximum in the surface vicinity before it decays as the distance from the surface increases. This is more pronounced as the heating period increases ($t \geqslant 2.5 \times 10^{-12}$ s). This occurs because of the amount of excess energy gain by the electrons and electron temperature distribution inside the substrate material. In this case, excess energy gain by the electrons due to irradiation field is considerably high in the longer heating duration and electron temperature decays sharply in the region next to the surface vicinity ($x > 2 \times 10^{-8}$ m). The effect of pulse shape on the entropy production is more pronounced for short heating durations ($t \leqslant 10^{-12}$ s). The maximum entropy produced inside the sub-

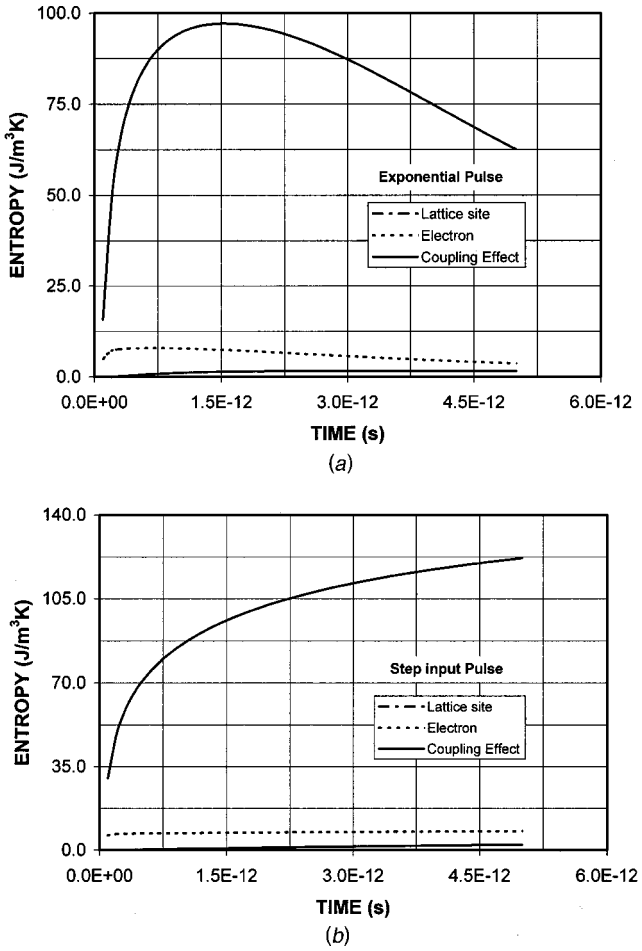

Fig. 7 Integrated entropy production inside the substrate material—(*a*) for exponential pulse, (*b*) for step input pulse

strate material due to exponential pulse is slightly higher than its counterpart corresponding to step input pulse shape.

2. The entropy production due to lattice system is similar to that produced due to electron system, provided that the amount of entropy produced is less. The entropy production occurs mainly in the surface region of the substrate material. This is due to lattice site temperature distribution below the surface. In this case, energy transfer by the electrons to the lattice site through collisional process is less during the picosecond heating duration. Consequently, temperature increase in the lattice site is small. The effect of pulse shape on the entropy production is significant; i.e., in the early heating period, entropy production corresponding to exponential pulse shape is more than that corresponding to step input pulse. This reverses as the heating period progresses further ($t \geqslant 5\times10^{-12}$ s).
3. The entropy production due to coupling process attains considerably larger values as compared to electron and lattice systems. The behavior of entropy curves is similar to that for electron system. The attainment of high entropy production is because of the potential energy and flux components in the energy production term, which increases with increasing heating period; i.e., electron temperature rises rapidly with increasing heating period, while rise in lattice site temperature is gradual. This results in large temperature difference between the electron and the lattice systems as the heating progresses. This enhances the potential energy and flux terms in the entropy equation. The effect of pulse shape on the entropy production is considerable. The amount of entropy production increases in the case of exponential pulse shape and the trend of the entropy curves inside the substrate material differs for different pulse shapes; i.e., step input pulse profile results in gradual decrease in entropy curves.
4. The integrated entropy production (integrated over the depth for a given time) increases rapidly in the early heating period, and it reduces as the heating period progresses in exponential pulse case, while it increases gradually in the step input pulse case. This indicates that integrated entropy profile almost follows the exponential pulse profile. The rapid rise of the integrated entropy production in the early heating period is because of the potential energy component in the entropy equation, which attains high values in the early heating period.

Acknowledgment

The author acknowledges the support of King Fahd University of Petroleum and Minerals, Dhahran, Saudi Arabia for this work.

Nomenclature

A = area where electrons flux (m^2)
ABS = absolute value
C_e = electron heat capacity (J/m^3K)
C_l = lattice heat capacity (J/m^3K)
Cp = specific heat of lattice site (J/kg.K)
ΔE = energy transferred to lattice site (J)
f = fraction of excess energy exchange
G = electron phonon coupling factor (W/m^3K)
g_j = no. of quantum states
I_o = laser peak power intensity (W/m^2)
J_q = flux term (W/m^3)
k = thermal conductivity (W/m.K)
k_B = Boltzmann's constant (1.38×10^{-23} J/K)
m_e = electron mass (kg)
N = electron no. density ($1/m^3$)
r_f = reflection coefficient
S = source term
s = spatial coordinates corresponding to electron movement (m)
s_{ent} = entropy production (J/m^3K)
$\dot{s}_e$ = entropy generation rate due to electron system (W/m^3K)
$\dot{s}_l$ = entropy generation rate due to lattice system (W/m^3K)
$\dot{s}_{el}$ = entropy generation rate due to coupling process (W/m^3K)
T_l = lattice site temperature (K)
T_e = electron temperature (K)
T_d = debye temperature (K)
t = time (s)
Δt = time increment (s)
u = internal energy (J)
V = electron mean velocity (m/s)
x = spatial coordinates corresponding to x-axis for phonon (m)
Δx = spatial increment (m)
α = thermal diffusivity (m^2/s)
β = pulse parameter (1/s)
δ = absorption coefficient (1/m)
χ = force term (1/K)
λ = mean free path of electrons (m)
ρ = density (kg/m^3)
τ_p = electron-phonon relaxation time (s)
τ_s = electron thermal relaxation time (s)

References

[1] Fujimoto, J. G., Liu, J. M., and Ippen, E. P., 1984, ''Femtosecond Laser Interaction With Metallic Tungsten and Nonequilibrium Electron and Lattice Temperatures,'' Phys. Rev. Lett., **53**, pp. 1837–1840.

[2] Elsayed-Ali, H. E., Norris, T. B., Pessot, M. A., and Mourou, G. A., 1987, ''Time-Resolved Observation of Electron-Phonon Relaxation in Copper,'' Phys. Rev. Lett., **58**, No. 12, pp 1212–1215.

[3] Eesley, G. L., 1986, ''Generation of Nonequilibrium Electron and Lattice Temperatures in Copper by Picosecond Laser Pulses,'' Phys. Rev. B, **33**, pp. 2144–2151.

[4] Qiu, T. Q., and Tien, C. L., 1994, ''Femtosecond Laser Heating of Multi-Layer Metals—I. Analysis,'' Int. J. Heat Mass Transf., **37**, No. 17, pp 2789–2797.

[5] Wang, X. Y., Riffe, D. M., Lee, Y. S., and Downer, M. C., 1994, ''Time-Resolved Electron-Temperature Measurement in a Highly Excited Gold Target Using Femtosecond Thermionic Emission,'' Phys. Rev. B, **50**, pp. 8016–8019.

[6] Tzou, D. Y., 1995, ''A Unified Field Approach for Heat Conduction From Macro-to-Micro-Scales,'' ASME J. Heat Transfer, **117**, pp. 8–16.

[7] Al-Nimr, M. A., and Arpaci, V. S., 1999, ''Picosecond Thermal Pulses in Thin Metal Films,'' J. Appl. Phys., **85**, pp. 2517–2521.

[8] Yilbas, B. S., 1986, ''Heating of Metals at a Free Surface by Laser Radiation an Electron Kinetic Theory Approach,'' Int. J. Eng. Sci., **24**, No. 8, pp. 1325–1334.

[9] Yilbas, B. S., and Shuja, S. Z., 1999, ''Laser Short-Pulse Heating of Surfaces,'' J. Phys. D, **32**, pp. 1947–1954.

[10] Sieniutycz, S., 1999, ''Carnot Problem of Maximum Work From a Finite Resource Interacting With Environment in a Finite Time,'' Physica A, **264**, pp. 234–263.

[11] Menshutina, N. V., and Darokhov, I. N., 1996, ''Simulation of Drying on the Basis of Nonequilibrium Thermodynamics of Heterogeneous Multiphase Polydispersed Systems,'' Drying Technol., **14**, pp. 915–921.

[12] Demirel, Y., and Sandler, S. I., 2001, ''Linear-Nonequilibrium Thermodynamics Theory for Coupled Heat and Mass Transport,'' Int. J. Heat Mass Transf., **44**, pp. 2439–2451.

[13] Yilbas, B. S., 1999, ''Three-Dimensional Laser Heating Model and Entropy Generation Consideration,'' ASME J. Energy Resour. Technol., **121**, pp. 217–224.

[14] Yilbas, B. S., and Sahin, A. Z., 1993, ''An Approach to Convergency of Kinetic Theory to Fourier Theory in Relation to Laser Heating Process,'' Jpn. J. Appl. Phys., **32**, Part 1, No. 12A, pp. 5646–5651.

[15] Corkum, P. B., Brunel, F., and Sherman, N. K., 1988, ''Thermal Response of Metals to Ultrashort-pulse Laser Excitations,'' Phys. Rev. Lett., **25**, pp. 2886–2889.

[16] Sonntag R. E., and Van Wylen G. J., 1976, Fundamentals of Statistical Thermodynamics, ''*Series in Thermal and Transport Sciences*, 1st Edited, John Wiley and Sons Inc., New York, NY.

[17] Smith G. D., 1985, *Numerical Solution of Partial Differential Equations: Finite Difference Methods*, 3rd Edition Clarendon Press, Oxford, UK.

Bekir Sami Yilbas *obtained his BS degree in Mechanical Engineering in 1976, and his M.Sc. and Ph.D. degrees in 1978 and 1981 from the Birmingham University in UK. He has been working on laser-induced processing including the machining analysis. His work extends from thermo-fluid science to manufacturing. He published over 200 journal papers and presented many papers in international conferences. He received The Present of India's Award in 1988, Science and Technology Award in 1990 from Science and Technology Foundation in Turkey, The Best Researcher Awards in 1997 and 2002 from King Fahd University of Petroleum and Minerals. He is on the Editorial Board of International Journal of Machine Tool and Manufacture Design, Research and Application and Journal of Materials Processing Technology. He is married with two children. He has been the member of many international scientific conferences.*